

Ultrathin Au Nanowires and Their Transport Properties

Chao Wang,[†] Yongjie Hu,[‡] Charles M. Lieber,^{*,‡} and Shouheng Sun^{*,†}*Department of Chemistry and Division of Engineering, Brown University, Providence, Rhode Island 02912, and
Department of Chemistry and Chemical Biology, Harvard University, Cambridge, Massachusetts 02138*

Received May 7, 2008; E-mail: cml@cmliris.harvard.edu; ssun@brown.edu

Fabrication of molecular-scale interconnects is key to achieve extremely dense logic and memory circuits.¹ Nanowires (NWs) are considered an essential component for these interconnects and have been used extensively to build nanoelectronic devices for applications in sensors,² waveguides,³ photonics,⁴ and piezoelectronics.⁵ Gold (Au) is chemically inert and has very low resistivity. These properties make Au NWs an ideal candidate as interconnects for linking molecular devices. Various methods have been developed to synthesize Au NWs. These include solution phase reduction of HAuCl₄ in a micellar structure formed either by CTAB in an aqueous solution,⁶ or by oleic acid/oleylamine in an organic solvent,⁷ reduction of HAuCl₄ in a nanoporous anodic aluminum oxide template⁸ or on other templates.⁹ Au NWs can also be fabricated via physical deposition of Au on a lithographically patterned substrate.¹⁰ Once formed, these Au NWs can be assembled onto a substrate via either the Langmuir–Blodgett technique,¹¹ or under an electric field.¹² However, Au NWs obtained in these approaches are polycrystalline and have rough surface. Transport studies have revealed that the resistivity of these polycrystalline Au NWs is higher than the bulk Au, and these NWs can only stand for a comparatively low current density ($\sim 10^{12}$ A/m² for 60 nm Au NWs) that drops precipitously at the diameters below 60 nm due to electromigration.¹³ There is no conclusive evidence on the origin of this high resistivity and low failure current density, which may arise from the electron wave function confinement at the nanometer scale, or from electromigration in the polycrystalline Au NWs. Here we report a facile synthesis of single crystalline ultrathin Au NWs with their diameters controlled in less than 10 nm. Transport study shows that the 9 nm Au NWs have a failure current density of 3.5×10^{12} A/m², indicating that the electromigration problem can be circumvented in ultrathin single-crystal NWs.

The Au NWs were synthesized by the reduction of HAuCl₄ in oleic acid (OA) and oleylamine (OAm). OAm serves both as a reducing agent and a stabilizer. In a typical synthesis of micrometer long Au NWs with 9 nm diameter, a solution (2 mL hexane and 2 mL OAm) of 0.2 g of HAuCl₄ was added to the mixture of OA (10 mL) and OAm (8 mL) at 80 °C under vigorous magnetic stirring. Hexane was evaporated under nitrogen atmosphere. Magnetic stirring was stopped after 5 min, and the solution was kept steady at this temperature for 5 h. The Au NWs were precipitated out by adding ethanol and centrifugation. The dark-red product was washed twice with ethanol and redispersed in hexane.

Figure 1 shows the representative transmission electron microscopy (TEM) images of the as-synthesized Au NWs with their diameter in 3 (Figure 1A) and 9 nm (Figure 1B) respectively. This diameter was tuned by controlling solvent combination during the synthesis. 3 nm Au NWs were made when only OAm was used as

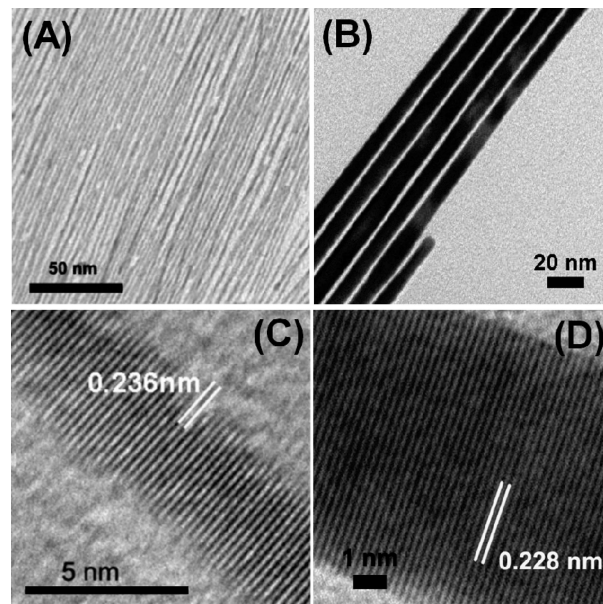


Figure 1. TEM images of (A) 3 nm Au NWs, (B) 9 nm Au NWs, and HRTEM images of (C) 3 nm NW, (D) 9 nm Au NW.

solvent, whereas 9 nm Au NWs were obtained from a mixture solvent of 10 mL OAm and 10 mL of OA. In all these syntheses, Au NWs were in micrometer long. High resolution TEM (HRTEM) images show the ordered crystal fringes perpendicular to the growth direction with relatively smooth wire surface (Figure 1C and D). The interfringe distances are measured to be 0.23–0.24 nm, corresponding to (111) lattice spacing (0.23 nm) of the face centered cubic (fcc) Au. The fcc structure of these Au NWs is further confirmed by X-ray diffraction (XRD) pattern of the NW assembly (Figure S1, Supporting Information).

The Au NWs are likely obtained from the micellar structure formed by self-assembly of OAm or OAm/OA from which the polar groups attract to each other and the hydrophobic chains are intercalated to give the alternating channel structure. OAm can bind to Au via its NH₂ group. Assuming the Au nuclei start as polyhedral shape, which is reasonable for fcc metal due to the minimum surface energy,¹⁴ OAm must bind preferentially to the (100) faces on the Au nuclei, and the one-dimensional Au growth along $\langle 111 \rangle$ direction is channeled by the micellar structure. This is similar to what has been predicted for the growth of Au, Ag and FePt NWs in the recent reports.¹⁵ This channel-mediated growth is further evidenced by controlled growth of Au NWs and Au nanoparticles under stirring conditions. Figure S2A (Supporting Information) shows a representative TEM image of the product obtained from growing the 3 nm Au NWs under a magnetic stirring condition (~ 600 rpm). It can be seen that the product contains high portion of Au nanoparticles (5–6 nm) with few Au NWs present in the mixture.

[†] Brown University.

[‡] Harvard University

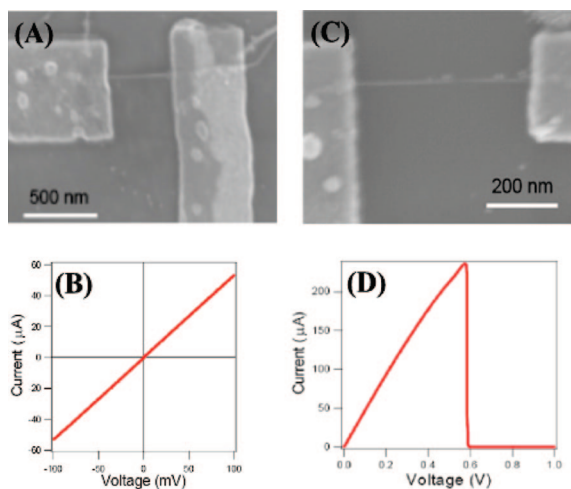


Figure 2. (A) SEM image of a 9 nm Au NW cross two patterned Au electrodes; (B) room-temperature I–V behavior of the 9 nm Au NW; (C) SEM image of the broken 9 nm Au NW; and (D) the break-down I–V behavior of the 9 nm Au NW.

In a separate test, the reaction solution was left undisturbed after adding the HAuCl_4 solution, and dominant product was Au NWs, as shown in Figure 1A. Similar results were obtained in the synthesis of 9 nm Au NWs. This implies that the growth of Au NWs is indeed from the one-dimensional micellar structure and mechanical stirring can destroy the one-dimensional structure, leading to the formation of nanoparticles.

To measure the transport properties of the as synthesized Au NWs, Au NWs from their hexane dispersion were deposited onto a SiO_2/Si substrate. E-beam lithography followed by evaporation of Cr/Au (5/50 nm) metal films was used to define the contacts. Figure 2A shows the scanning electron microscopy (SEM) image of the substrate with the 9 nm Au NWs assembled on its surface. The room temperature I–V data is given in Figure 2B, from which one can see that the NW as an electron conductor exhibits the conventional ohmic behavior. For the 9 nm NW with the length of 450 nm, the resistance was measured to be $1.85 \text{ k}\Omega$ (no contact resistance correction). This corresponds to the resistivity of $260 \Omega \cdot \text{nm}$, much lower than that measured from polycrystalline Au NWs ($1000 \Omega \cdot \text{nm}$).^{9a}

The 9 nm NW broke down when the voltage applied on the NW was raised to 0.58 V. Figure 2C shows the SEM image of the broken NW between two electrodes and Figure 2D is the I–V curve of the NW exhibiting breakdown behavior. The breakdown current density was measured to be $3.5 \times 10^{12} \text{ A/m}^2$. This value is higher than that measured from the Au NWs fabricated from either lithography or DNA template – the failure current densities reach $1.0 \times 10^{12} \text{ A/m}^2$ for the 60–800 nm Au NWs but drop precipitously for those smaller than 60 nm.¹³ The low failure current densities observed from the polycrystalline Au NWs are attributed to electromigration that occurs preferentially at crystal grain boundaries. It has been predicted that elimination of these grain boundaries can increase the failure current densities in small NWs.¹³ This is clearly seen in the 9 nm Au NWs. With their single crystalline nature, these 9 nm NWs are free of energy dissipation and void diffusion at the grain boundary or defect sites, giving high failure current densities. The study proves that ultrathin metallic nanowire interconnects should function as well as their larger counterparts, provided that they are essentially single crystalline.

The transport measurements further show that the single-crystal Au NWs without the presence of grain boundaries can support a

very high current flow. From Figure 2D, we can see the maximum current that flows through the 9 nm Au NW reaches $250 \mu\text{A}$. This is comparable to the failure current of multiwall CNT (10 nm in diameter) devices with a wall-by-wall breakdown current at $200 \mu\text{A}^{16}$ (about $20 \mu\text{A}$ for single-wall CNT).¹⁷ The failure current of Si NWs is much higher, but the working current of transistors based on Si NWs is only in the order of 100 nA.¹⁸ The resistance of the Au NW is also small compared to the CNT and SiNW (usually in the order of $\text{M}\Omega$), implying great potential of these Au NWs as interconnects for nanoelectronic applications.

In conclusion, this paper presents a facile synthesis of single-crystalline Au NWs by reduction of HAuCl_4 in oleic acid and oleylamine. These micrometer-long NWs have been prepared with controlled diameters of either 3 or 9 nm, and the diameter could be further tuned within this regime by varying the volume ratio of oleylamine and oleic acid. When linked between two gold electrodes, the 9 nm Au NW shows good electron conductivity with its resistivity at $260 \Omega \cdot \text{nm}$, breakdown current at $250 \mu\text{A}$ and failure current density reaching $3.5 \times 10^{12} \text{ A/m}^2$. The study indicates that the chemically made ultrathin single crystalline Au NWs can be used as a molecular-scale interconnect for nanoelectronic applications.

Acknowledgment. The work was supported by NSF/DMR 0606264.

Supporting Information Available: Au nanowire characterization. This material is available free of charge via the Internet at <http://pubs.acs.org>.

References

- (1) Lu, W.; Lieber, C. M. *Nat. Mater.* **2007**, *6*, 841–850.
- (2) (a) Cui, Y.; Wei, Q.; Park, H.; Lieber, C. M. *Science* **2001**, *293*, 1289–1292. (b) Zheng, G.; Patolsky, F.; Cui, Y.; Wang, W. U.; Lieber, C. M. *Nat. Biotechnol.* **2005**, *23*, 1294–1301. (c) McAlpine, M. C.; Ahmad, H.; Wang, D.; Heath, J. R. *Nat. Mater.* **2007**, *6*, 379–384.
- (3) (a) Johnson, J. C.; Choi, H.; Knutsen, K. P.; Schaller, R. D.; Yang, P.; Saykally, R. J. *Nat. Mater.* **2002**, *1*, 106–110. (b) Tong, L.; Gattass, R. R.; Ashcom, J. B.; He, S.; Lou, J.; Shen, M.; Maxwell, I.; Mazur, E. *Nature* **2003**, *426*, 816–819. (c) Law, M.; Sirbulu, D. J.; Johnson, J. C.; Goldberger, J.; Saykally, R. J.; Yang, P. *Science* **2004**, *305*, 1269–1273. (d) Barrelet, C. J.; Greytak, A. B.; Lieber, C. M. *Nano Lett.* **2004**, *4*, 1981–1985.
- (4) (a) McAlpine, M. C.; Friedman, R. S.; Jin, S.; Lin, K.; Wang, W. U.; Lieber, C. M. *Nano Lett.* **2003**, *3*, 1531–1535. (b) McAlpine, M. C.; Friedman, R. S.; Lieber, C. M. *Proc. IEEE* **2005**, *93*, 1357–1363. (c) Nakayama, Y.; Pauzauskis, P. J.; Radenovic, A.; Onarato, R. M.; Saykally, R. J.; Liphardt, J.; Yang, P. *Nature* **2007**, *447*, 1098–1102.
- (5) Wang, Z. L.; Song, J. *Science* **2006**, *312*, 242–246.
- (6) Krichevski, O.; Tirosh, E.; Markovich, G. *Langmuir* **2006**, *22*, 867–870.
- (7) Halder, A.; Ravishankar, N. *Adv. Mater.* **2007**, *19*, 1854–1858.
- (8) Forrer, P.; Schlottig, F.; Siegenthaler, H.; Textor, M. *J. Appl. Electrochem.* **2000**, *30*, 533–541.
- (9) (a) Song, J. H.; Wu, Y.; Messer, B.; Kind, H.; Yang, P. *J. Am. Chem. Soc.* **2001**, *123*, 10397–10398. (b) Karim, S.; Toimil-Molares, M. E.; Maurer, F.; Miehe, G.; Ensinger, W.; Liu, J.; Cornelius, T. W.; Neumann, R. *Appl. Phys. A: Mater. Sci. Process.* **2006**, *84*, 403–407.
- (10) Sheats, J. R.; Smith, B. W. *Microolithography: Science and Technology*; CRC Press: Boca Raton, FL, 1998.
- (11) Huang, J.; Fan, R.; Connor, S.; Yang, P. *Angew. Chem., Int. Ed.* **2007**, *46*, 2414–2417.
- (12) Duan, X.; Huang, Y.; Cui, Y.; Wang, J.; Lieber, C. M. *Nature* **2001**, *409*, 66–69.
- (13) (a) Durkan, C.; Schneider, M. A.; Welland, M. E. *J. Appl. Phys.* **1999**, *86*, 1280–1286. (b) Aherne, D.; Satti, A.; Fitzmaurice, D. *Nanotechnology* **2007**, *18*, 125205.
- (14) Romanowski, W. *Surf. Sci.* **1969**, *18*, 373–388.
- (15) (a) Sun, Y.; Gates, B.; Mayers, B.; Xia, Y. *Nano Lett.* **2002**, *2*, 165–168. (b) Caswell, K. K.; Bender, C. M.; Murphy, C. J. *Nano Lett.* **2003**, *3*, 667–669. (c) Wang, C.; Hou, Y.; Kim, J.; Sun, S. *Angew. Chem., Int. Ed.* **2007**, *46*, 6333–6335.
- (16) Yuzvinsky, T. D.; Mickelson, W.; Aloni, S.; Konsek, S. L.; Fennimore, A. M.; Begtrup, G. E.; Kis, A.; Regan, B. C.; Zettl, A. *Appl. Phys. Lett.* **2005**, *87*, 83103.
- (17) Pop, E.; Mann, D. A.; Goodson, K. E.; Dai, H. *J. Appl. Phys.* **2007**, *101*, 93710.
- (18) Cui, Y.; Lieber, C. M. *Science* **2001**, *291*, 851–853.

JA803408F